Dynamics of Multiple Slip and Thermal Radiation on Hydromagnetic Casson Nanofluid Flow over a Nonlinear Porous Stretchable Surface

O. E. Omotola[1] and E. O. Fatunmbi[2*]

[1] *Poly International College, Ilaro, Nigeria.*
[2] *Department of Mathematics and Statistics, Federal Polytechnic, Ilaro, Nigeria.*

Authors' contributions

This work was carried out in collaboration between both authors. Author EOF designed the study, formulation and Mathematical Modelling of the problem and wrote the first draft of the manuscript. Author OEO provided solution and validation of the problem, interpreted and discussed the results as well as the literature searches. Both authors read and approved the final manuscript.

Original Research Article

ABSTRACT

Aims/ Objectives: This paper examines the dynamics of multiple slip together with thermal radiation effects on the transport of a magnetohydrodynamic Casson nanofluid passing a nonlinear porous stretchable sheet in the existence of viscous dissipation and chemical reaction.
Study Design: Cross-sectional study.
Methodology: The outlining equations modeling the transport phenomenon are simplified into nonlinear ordinary differential equations via the approach of similarity transformations and subsequently analyzed numerically by shooting techniques alongside Runge-Kutta Fehlberg scheme.
Results: The outcomes of decisive parameters affecting the flow, heat, and nanoparticle concentration are graphically deliberated. From the investigation, it is revealed that Brownian motion, viscous dissipation, and thermophoresis parameters augment the thermal boundary layer and propel an upward growth in the temperature profile. Furthermore, the slip factor decelerates the flow and heat dissipation while the fluid movement drags in the existence of the magnetic field.

Corresponding author: E-mail: ephesus.fatunmbi@federalpolyilaro.edu.ng;

Conclusion: The results obtained in this study compared favourably well with existing related studies in literature under limiting scenarios.

1 INTRODUCTION

Newton's law of viscosity does not govern many industrial and manufacturing processing fluids like ceramics, inks, liquid detergents, syrups, mixed oils, gypsum pastes, polymers, hair colors, fruit juices, etc. These liquids constantly change their viscosity under shear tension, which makes them fall under non-Newtonian fluids category. Since these fluids have varying thermophysical attributes, establishing them using a single constitutive equation is perturbing [1-2]. Thus, in the literature, various concepts or models of these fluids have been formulated and discussed. The values and defects of each non-Newtonian fluid model are unique. For instance, Karra et al. [3] explained that the non-Newtonian Maxwell model tends to predict the results of fluid relaxation time among the simplest rate models. Similarly, Ireka and Okoya [4] further described the second-grade fluid as another form of non-Newtonian fluids by considering the impacts of viscous and elastic effects on the fluid flow. Fatunmbi and Fenuga [5] deliberated on the transport of micropolar fluid as a branch of non-Newtonian fluid with non-symmetric stress tensor.

Furthermore, Casson [6] established the Casson fluid concept as another form of the non-Newtonian fluid model. This is a standard viscoelastic model in many fluids like blood, tomato sauce, honey, etc. This model displays yield stress and acts as solid if the shear strength is far less than the yield stress. Conversely, it distorts when the shear stress is more significant than the yield stress in performance [7-8]. Casson fluid is a more effective cooling agent than many other fluids and thus has attracted the interest of many scientists. In view of various applications, the model of Casson fluid has been reported by various authors on different configurations, conditions and parameters. Shaw et al. [9] explore the results of various Casson fluid flow emerging parameter on flat convective surface conditions. Similarly, Asogwa and Ibe [10] discussed the transport of magnetodynamics Casson fluid in a porous sheet with emphasis on the heat-mass transfer aspect while Shamshuddin et al. [11] numerically calculated the impact of chemical reaction on the motion of Casson fluid over an inclined plate.

Today, nanofluids are used in place of traditional fluids (such as; water, oil, ethylene-glycol and so on) because they display soaring thermal conductivity. The development of nanofluids provides a high temperature transfer and lessens heat transfer of energy consumption devices. The first investigator to develop fluids that include the nanosize nanofluids suspension is Choi [12]. Afterward, Lee et al. [13] extended this study by reporting that the nanofluids have excellent heat transfer properties relative to the basic fluids. Many researchers subsequently suggested improved thermophysical properties relative to the conventional fluids alongside heat distribution of nanofluids. Buongiorno [14] also expanded the rationale for improving the thermal performance of nanofluids. Correspondingly, the improvement of thermal conductivity of different concentrations of nanoparticles was examined by Aybar et al. [15]. They concluded that adding nanoparticles to fluids enhances thermal conductivity in the boundary layer. Similarly, Okonkwo et al. [16] highlighted an extensive analysis of nanofluids in different heat transfer applications. Their results depicted a situation where the heat transfer of base fluids is lower than that of nanoparticles. Further analysis of Brownian movement and thermophoresis effects on nanofluids was conducted by Abdelmalek et al. [17]. Additionally, Makinde et al. [18] numerically studied magnetohydrodynamic nanofluid convective heat transfer problem along

a stretched plate characterized by varying viscosity and radiation effect. Alreshidi et al. [19] analyzed the nanofluid concept by integrating the effect of Brownian movement and thermophoresis using Lie group analysis. Also, Ashraf [20] studied the effects of a nanofluids normal convective flow over the vertical plate with special attention given the influence of variable liquid properties. Recently, the motion of Powell-Eyring fluid blended with nanoparticles characterized by exponential varying viscosity over a nonlinear vertical Riga plate was investigated by Fatunmbi and Adeosun [21]. Nevertheless, the phenomenon of slip at the wall was not considered in the aforementioned studies.

Slip effects have drawn the attention of scientists over the last decade due to their consequential usage in diverse engineering processes. In many industrial processes, namely: microscale and nanoscale devices, both velocity slip and the wall temperature jump have many influences. Navier [22] investigated the slip boundary condition and prescribed the speed aligns with the shear stress on the wall. Thereafter, several scientists have studied the slip effects in speed and a wall temperature jump in various geometries containing viscous fluids and nanofluids in depth. Rashad [23] incorporated the finite-difference technique to examine significance of slip on unsteady three-dimensional flow. The findings suggested that raising the velocity slip variable significantly reduced the shear stress as well as heat transfer. Similarly, the impact of slip with heat transfer characteristics in a permeable enclosure was considered by Afifys *et al.* [24] using Lie symmetry analysis. Additionally, Uddin *et al.* [25] recently applied temperature and mass convective boundary conditions to obtain practical effects of slip condition. The analysis demonstrated that expanded hydrodynamic slip lightens skin tension and enhances the local Nusselt number. Fatunmbi and Fenuga [26] analyzed such a problem on the flow of magneto-micropolar fluid over an exponentially stretched plate. The authors reported a decreased heat transfer as a result of thermal slip in the heat dissipation equation. Also, slip influence on chemically reactive micropolar fluid flow was investigated by Fatunmbi and Adeniyan [27] with

the report that a boost in the strength of the slip factor decelerates the locomotion of the fluid.

Thermal radiation effects contribute to many practical applications in physics and engineering during heat transfer. In space exploration and high heating systems, radiation is a form of heat transfer for many industrial and radiological products. For instance, thermal radiation can be critical in controlling thermal performance for polymer processing industries. Consequently, the performance of a production process in this state is bent on heat control factors. High-temperature plasma, cooling nuclear power plants, metallic gases, and electric-generating devices are practical applications for radiative heating transfer from a vertical surface through conductive grey fluids [28]. However, the impact of radiation as heat transfer on the thermal boundary layer is still yet to be fully explored. Jamaluddin *et al.* [29] evaluated the impact of radiation on the heat performance features of ferrofluid in the stagnation field using the collocation method. Likewise, Zaidi *et al.* [30] explored such a problem on a vertical plate of electroconductive couple force fluid.

In several fields related to engineering science, the impacts of a chemical reaction are an essential consideration in studying heat-mass transfer problems. Bhandari [31] numerically studied the time-independent problem of a reactive micropolar nanofluid transport confined in two-dimensional enclosure with particle rotation. According to the report, fluid temperature advances as the chemical reaction rate improves. Similarly, this report was verified by Abd El-Aziz [32] by employing a transport model of time-dependent chemical reaction on two-dimensional nanofluid flow caused by the time-dependent surface temperature and concentration. Furthermore, Fatunmbi and Adeniyan [33] numerically solved such a problem on the motion of electroconductive micropolar fluid near a stagnation point while Eid [34] investigated Sherwood number as a growing feature of a reaction rate in the study of chemical reaction effect on the magnetohydrodynamic nanofluid flow over a stretching surface. More so, Afify and Elgazery [35] analyzed the influence of chemical reaction on MHD nanoparticle

fluids physical processes. It was observed that destructive chemical reactions enhance multiphase flow rates and weaken them in the nanofluid concentration.

The aforementioned studies have however been conducted over a linearly stretchable surface without considering a nonlinear surface. For practical purposes such as in wire drawing, the stretching velocity assumes nonlinearity. Hence, the current study intends to investigate the dynamics of multiple slips and thermal radiation on the transport of an electroconductive nanofluid past a nonlinear permeable stretching surface. The physical model incorporates the influence of chemical reaction together with viscous dissipation associated with heat generation/absorption. Numerical results of the emerging physical terms on the dimensionless quantities, namely: velocity, temperature, and concentration fields are described graphically and discussed. This study has verified the numerous practical uses of nanoparticles embedded in a Casson fluid, predominantly in biomedical, chemical manufacturing, microelectronics, and nuclear reactors processes.

2 PROBLEM FORMULATION AND ANALYSIS

The Casson-nanofluid transport is assumed to be steady, incompressible and configured in a two-dimensional porous nonlinear stretchable surface. The flow is characterized by multiple slip properties, heat dissipation, homogeneous chemical reaction, thermophoresis and Brownian movement of the nanoparticles. The flow occurs at region $y \geq 0$, with y being the coordinate measured to the stretching surface. Also, perpendicular to the surface is a variable external magnetic field $B(x) = \frac{B_0}{x^{(1-n)/2}}$ ([36-38]) while ignoring the impact of the induced magnetic field. The momentum equation also contains a non-uniform porous medium permeability expressed as $k_p(x) = K_0 x^{(1-n)}$ ([37, 39]). The stretching sheet generates the fluid flow at $(x = y = 0)$. It is supposed that the sheet varies in nonlinear manner with range x from the direction of flow $(u_w = ax^n$ as indicated in Fig. 1), where a and n respectively symbolize a positive constant and nonlinear stretching term. A prescribed surface mass flux $v_w = \frac{v_0}{x^{(1-n)/2}}$ ([40-41]) is applied to the permeable sheet, $v_w > 0$ indicates injection while $v_w < 0$ denotes suction and v_0 is a constant (see Yazdi).
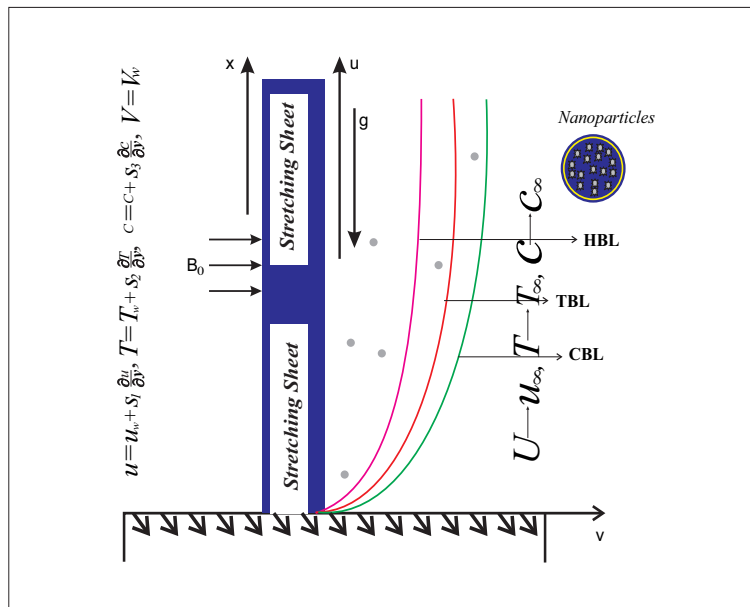
Fig. 1. Geometry of Flow

2.1 The Governing Equations

The rheological equation for flow of Casson fluid is expressed as follows (see Gbadeyan *et al.* [42], and Animasaun *et al.* [43]):

$$\tau_{ij} = 2(\mu_B + p_y/\sqrt{2\pi})e_{ij}, \pi > \pi_c \tag{1}$$

$$\tau_{ij} = 2(\mu_B + p_y/\sqrt{2\pi})e_{ij}, \pi > \pi_c \tag{2}$$

From equations (1-2), $\pi = e_{ij}$, where e_{ij} indicates the $(i,j) - th$ deformation rate constituent, π denotes the product of the deformation rate with itself, π_c denotes the critical value of the product, μ_B and p_y correspondingly define dynamic plastic viscosity and the yield stress. With the above-listed assumptions together with the Oberbeck-Boussinesq approximation, the transport equations are communicated as (Raza *et al* [44]):

$$\frac{\partial u}{\partial x} + \frac{\partial v}{\partial x} = 0, \tag{3}$$

$$u\frac{\partial u}{\partial x} + v\frac{\partial u}{\partial y} = \nu\left(1 + \frac{1}{\beta}\right)\frac{\partial^2 u}{\partial y^2} - \frac{\sigma B^2(x)}{\rho}u - \frac{\nu}{k_p(x)}u + g\beta_T(T - T_\infty) + g\beta_c(C - C_\infty), \tag{4}$$

$$u\frac{\partial T}{\partial x} + v\frac{\partial T}{\partial y} = \alpha\frac{\partial^2 T}{\partial y^2} + \tau\left[D_B\frac{\partial C}{\partial y}\frac{\partial T}{\partial y} + \frac{D_T}{T_\infty}\left(\frac{\partial T}{\partial y}\right)^2\right] + \frac{\mu}{\rho c_p}\left(1 + \frac{1}{\beta}\right)\left(\frac{\partial u}{\partial y}\right)^2 - \frac{1}{\rho c_p}\frac{\partial q_r}{\partial y} +$$
$$\frac{\sigma B^2(x)}{\rho c_p}u^2 + \frac{\nu}{c_p k_p(x)}u^2 + \frac{Q_o}{\rho c_p}(T - T_\infty), \tag{5}$$

$$u\frac{\partial C}{\partial x} + v\frac{\partial C}{\partial y} = D_B\frac{\partial^2 C}{\partial y^2} + \frac{D_T}{T_\infty}\frac{\partial^2 T}{\partial y^2} - K_r(C - C_\infty). \tag{6}$$

The controlling equations are constraint at the wall by:

$$u = u_w + S_1\frac{\partial u}{\partial y}, \ v = \pm v_w, \ T = T_w + S_2\frac{\partial T}{\partial y}, \ C = C_w + S_3\frac{\partial C}{\partial y} \ at \ y = 0,$$
$$u \to 0, \ T \to T_\infty, \ C \to C_\infty \ as \ y \to \infty. \tag{7}$$

In Eqs (3-7), x, y depicts cartesian coordinates alongside with u, v as respective velocity components. Likewise, the symbols ρ, ν, B_0 and σ are the fluid density, kinematic viscosity, magnetic field strength, and the electrical conductivity respectively. Also, $\beta_T(\beta_c)$, β, α, $T(C)$, $T_\infty(C_\infty)$ and g denote coefficient of thermal(solutal) expansion, Casson fluid term, thermal diffusivity, fluid temperature (concentration), ambient fluid temperature(concentration) and gravitational acceleration. Furthermore, k_p defines permeability of the porous medium, q_r is the radiative factor, $Q_o = Q_1 x^{n-1\cdot}$ indicates variable volumetric heat generation/absorption. The Brownian diffusion, thermophoretic diffusion as well as heat capacity of the fluid are denoted by D_B, D_T, (c_p). Similarly, $S_1 = S_4 x^{(1-n)/2}$, $S_2 = S_5 x^{(1-n)/2}$ and $S_3 = S_6 x^{(1-n)/2}$ respectively indicates the velocity, temperature and concentration slip factor sequentially. Besides, v_w implies the suction whereas $T_w(C_w)$ typifies temperature (concentration) at the sheet.

Using the Rosseland approximation,

$$q_r = -\left(\frac{4\sigma^*}{3k^*}\right)\frac{\partial T^4}{\partial y}, \tag{8}$$

with σ^* and k^* representing the Stefan-Boltzmann constant and mean absorption coefficient. Expanding T^4 in Taylor's series under the assumption that the flow temperature difference is low, then

$$T^4 \approx 4T_\infty^3 - 3T_\infty^4. \tag{9}$$

2.2 The Transfomed Equations

The following dimensionless quantities are introduced [44]

$$u = ax^n f'(\eta), \; v = -ax^{\frac{n-1}{2}} \left(\frac{\nu}{a}\right)^{\frac{1}{2}} \left(\frac{n+1}{2} f(\eta) + \frac{n-1}{2} \eta f'(\eta)\right), \; \eta = \left(\frac{a}{\nu}\right)^{\frac{1}{2}} x^{\frac{n-1}{2}} y,$$

$$T = (T_w - T_\infty)\theta(\eta) + T_\infty, \; C = (C_w - C_\infty)\phi(\eta) + C_\infty. \tag{10}$$

Imposing Eq. (10) into the main equations, Eq. (3) is satisfied while Eqs. (4-6) together with boundary conditions (7) yield the underlisted ordinary differential equations (11-14):

$$\left(1 + \frac{1}{\beta}\right) f''' + \frac{n+1}{2} ff'' - nf'^2 - (H + Da)f' + Gr\theta + Gc\phi = 0, \tag{11}$$

$$(1 + N_r)\theta'' + \frac{n+1}{2} Prf\theta' + \left(1 + \frac{1}{\beta}\right) EcPrf''^2 + PrHEcf'^2 + Pr(N_b\theta'\phi' + N_t\theta'^2) +$$

$$+ DaEcPrf'^2 + PrQ\theta = 0, \tag{12}$$

$$\phi'' + \frac{n+1}{2} Lef\phi' + \frac{N_t}{N_b}\theta'' - K_r\phi = 0, \tag{13}$$

$$f(0) = f_w, \; f'(0) = 1 + G_1 f''(0), \; \theta(0) = 1 + G_2\theta'(0), \; \phi(0) = 1 + G_3\phi'(0),$$

$$f' \longrightarrow 0, \; \theta \to 0, \; \phi \to 0 \; as \; \eta \to \infty. \tag{14}$$

In the above equation, K_r defines the chemical reaction parameter, Da implies Darcy parameter, G_1, G_2, G_3 orderly symbolizes the velocity, temperature and concentration slip parameter, H represent magnetic field parameter, Q describes the dimensionless heat source/sink, Le is the Lewis number, Gr denotes the Grashof number, N_b defines Brownian motion, N_t symbolizes thermophoresis term, Gc stands for solutal Grashof number, Ec signifies Eckert number, f_w symbolizes suction/injection parameter, Pr denotes the Prandtl number. Eq. (15) gives the details description of these parameters:

$$Pr = \frac{\nu}{\alpha}, \; H = \frac{\sigma B_0^2}{\rho a}, \; Le = \frac{\nu}{D_B}, \; N_b = \frac{(\rho c)_p D_B C_\infty}{(\rho c)_f \nu}, \; G_c = \frac{g\beta_c(c_w - c_\infty)}{a^2 x^{2n-1}},$$

$$N_t = \frac{(\rho c)_p D_T(T_f - T_\infty)}{(\rho c)_f T_\infty \nu}, \; f_w = -\frac{2v_0}{n+1}\sqrt{\left(\frac{1}{a\nu}\right)}, \; G_1 = S_4\sqrt{\frac{a(n+1)}{2\nu}},$$

$$Q = \frac{Q_1}{a\rho c_p}, \; Ec = \frac{u_w^2}{c_p(T_w - T_\infty)}, \; G_r = \frac{g\beta_T(T_w - T_\infty)}{a^2 x^{2n-1}}, \; Da = \frac{\nu}{ak_0}, \tag{15}$$

$$N_r = \frac{16\sigma^* T_\infty^3}{3k^* k}, \; G_2 = S_5\sqrt{\frac{a(n+1)}{2\nu}}, \; G_3 = S_6\sqrt{\frac{a(n+1)}{2\nu}}.$$

2.3 Quantities of Engineering Interest

The quantities of interest in this study for engineering purposes are sequentially presented in Eq. (16), the first being the skin friction coefficient (Cf_x), the second indicates the Nusselt number (Nu_x) while the third connotes the Sherwood number (Sh_x):

$$Cf_x = \frac{\tau_w}{\rho(u_w)^2}, \; Nu_x = \frac{xq_w}{k(T_w - T_\infty)}, \; Nu_x = \frac{xq_m}{D_B(C_w - C_\infty)} \tag{16}$$

where

$$\tau_w = \mu\left(1 + \frac{1}{\beta}\right)\frac{\partial u}{\partial y}\bigg|_{y=0}, \; q_w = -\left(k + \frac{16\sigma^* T_\infty^3}{3k^*}\right)\frac{\partial T}{\partial y}\bigg|_{y=0}, \; q_m = -D_B \frac{\partial C}{\partial y}\bigg|_{y=0} \tag{17}$$

The non-dimensional physical quantities are:

$$Re^{\frac{1}{2}} Cf_x = \left(1 + \frac{1}{\beta}\right) f''(0), \; Re^{-\frac{1}{2}} Nu_x = -(1 + N_r)\theta'(0), \; Re^{-\frac{1}{2}} Sh_x = -\phi'(0). \tag{18}$$

3 NUMERICAL SOLUTION AND RESULTS VALIDATION

The solution to the set of Eqs. (11-13) together with boundary condition (14) was sought numerically due to the nonlinearity of the problem. The popular shooting technique cum Runge-Kutta Fehlberg method was employed for the numerical integration. We did not publicize the technique here due to its popularity, however, the details of this technique can be found in Refs [45-47]. Except otherwise stated in the respective graphs, the following values have been fixed for the emerging parameters in the current study; $Nr = fw = K_r = 0.3, N_b = N_t = Da = K = H = 0.5, Gr = 0.70 = Gc, Q = 0.3 = \beta, n = 0.7, Ec = 0.1, Pr = 0.72, Le = 1.0, G_1 = 0.3 = G_2 = G_3$. Table 1 records the comparison of the present results with the published data of Gorla and Sidawi [48] and Megahed [49] under limiting conditions. From the table, it is clearly shown that there is a good agreement between the current results and those existing data in the absence of the concentration field, thermophoresis and Brownian motion, no slip condition and other limiting situations as described in the table.

4 RESULTS AND DISCUSSION

This section also highlights the reactions of different physical parameters, namely: thermophoresis parameter N_t, nonlinear stretching parameter n, chemical reaction K_r, Darcy parameter Da, momentum slip parameter G_1, solutal Grashof number G_c, concentration slip parameter G_3, Radiation term N_r, Brownian motion term N_b, Casson parameter β, magnetic field parameter H, Grashof number G_r, heat slip parameter G_2, heat source/sink Q on the non-dimensional velocity, temperature and concentration fields.

Fig. 2 depicts the attributes of β and H with respect to the velocity when other emerging parameters are fixed. The plot reveals that a rise in β produces a steady decrease in the velocity. It is noted that as β improves, a kind of resistive force in created in the flow region leading to a fall in the hydrodynamic boundary layer thickness and thereby a decelerated flow. With a rise in β, there is enhancement in the dynamic viscosity and consequently a decrease in the yield stress. This rise in the dynamic viscosity creates a resistance to the locomotion of the fluid as shown in the figure. Similarly, a resistive force named Lorentz force which opposes the fluid motion is induced by a rise in H due to the electroconductive nature of the Casson fluid. Thereby, the fluid motion decreases as the magnitude of H improves. In this scenario, the Lorentz force is generated when the magnetic field is normal to the flow of an electroconductive fluid. This gives the force an appropriate tendency to oppose the flow. The impact of nonlinear stretching term n and temperature slip parameter G_2 on the velocity profile is showcased in Fig. 3. Here an, enhancement in both n and G_2 decelerate fluid motion and the hydrodynamic boundary layer structure.

Table 1. Comparative analysis of $Re^{-\frac{1}{2}} Nu_x$ for variation in Pr with published studies when $Ec = Nr = H = Da = G_2 = N_t = Q = 0, \beta \to \infty, n = 1$

Pr	Gorla & Sidawi [48]	Megahed [49]	Present
2.0	0.91142	0.911358	0.911357
7.0	1.89046	1.895453	1.895403
10.0	2.30350	-	2.308003
20.0	3.35391	3.353902	3.353904
50.0	5.42474	-	5.424305
70.0	6.46221	-	6.462199
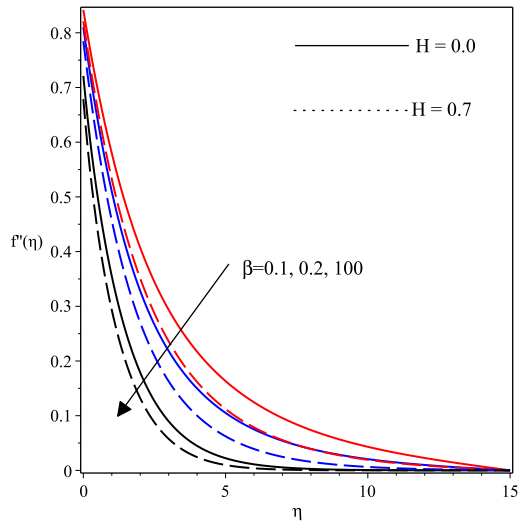
Fig. 2. Behaviour of β and H on $f'(\eta)$
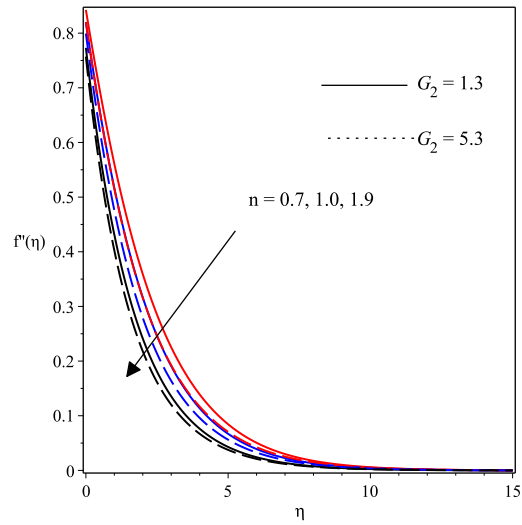
Fig. 3. Reaction of n and G_2 on $f'(\eta)$
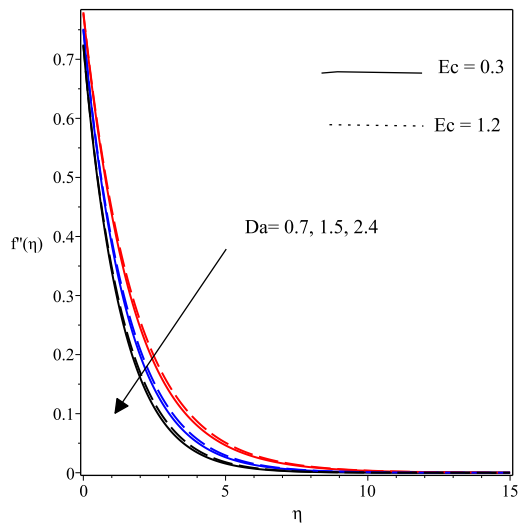
Fig. 4. Influence of Da and Ec on $f'(\eta)$
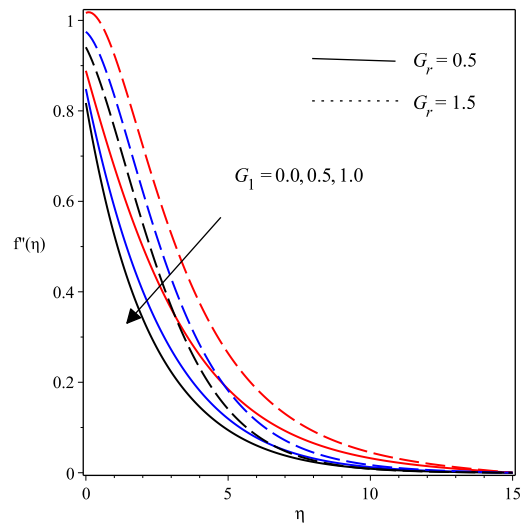
Fig. 5. Influence of G_1 and G_r on $f'(\eta)$

Fig. 4 describes the impact Darcy term Da in the presence of Ec on the flow field. The graph depicts increasing the magnitude of Da lowers the motion of the fluid. Consequently, permeability strengthens the resilience of the porous medium which mitigates fluid velocity. However, Ec exhibits the opposite pattern in this case as a rise in Ec reduces the fluid viscosity and thereby favours the speed of the fluid. The impacts of the momentum slip parameter G_1 and Grashof number G_r are displayed in Fig.

5. With escalating values of G_1, the velocity profile decreases. Here, the momentum supplied by the nonlinear stretchable surface is partially transferred to the fluid such that there is a decrease in the fluid motion. In the presence of G_r however, there is enhancement in the fluid motion as growth G_r boosts buoyancy force boosts while decreasing the viscous force. From Fig. 6, the impacts of G_c on the velocity field is similar to that of G_r in the flow field.
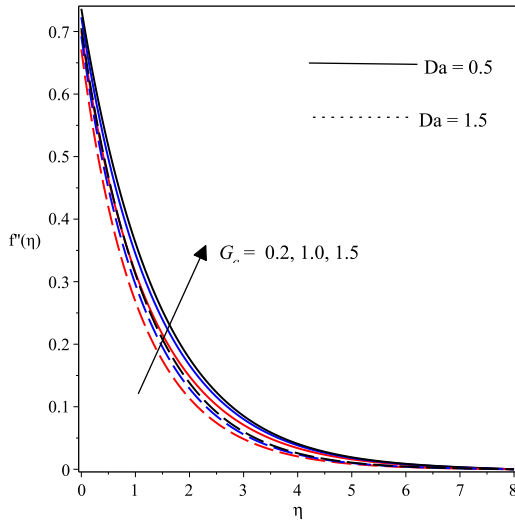
Fig. 6. Impact of G_c and Da on $f'(\eta)$ **Fig. 7. Plot of N_r and Pr on $\theta(\eta)$**
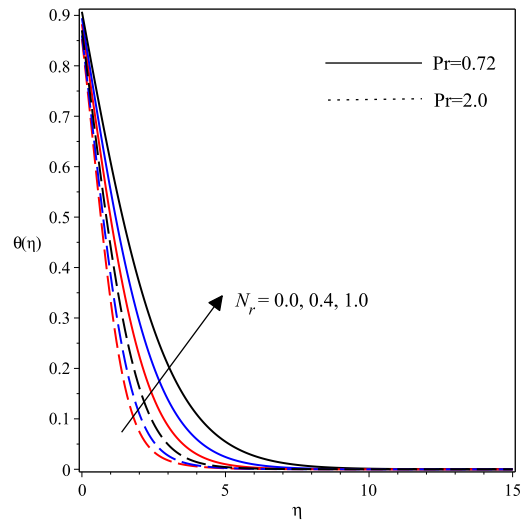
The combined impacts of N_r and Pr with respect to temperature field clearly informs that an improvement in Pr significantly reduces temperature as described in Fig. 7. The thermal boundary layer structure diminishes as Pr rises in magnitude due to a fall in thermal conduction of the fluid. Hence, the temperature significantly falls as depicted in the figure. On the contrary, the rising values of N_r displays upward movement on the dimensionless temperature profile. Here, increasing the radiation parameter triggers a spike in temperature due to reduction in the mean absorption coefficient in the radiative heat flux. The plot of temperature distribution versus η for diverse values of heat source term Q in the presence of nonlinear stretching parameter n is illustrated in Fig. 8.
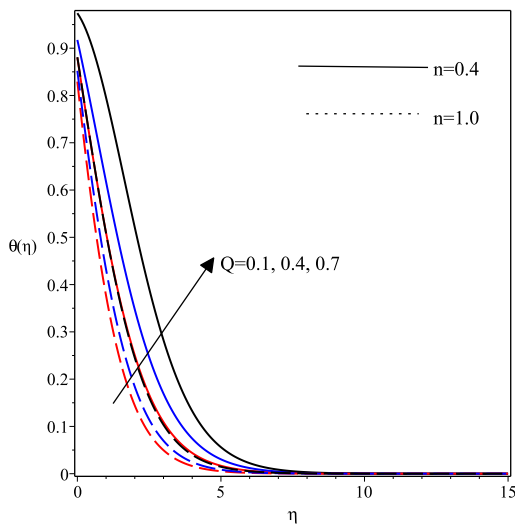
Fig. 8. Effects of Q and n on $\theta(\eta)$ **Fig. 9. Impacts of N_b and M on $\theta(\eta)$**
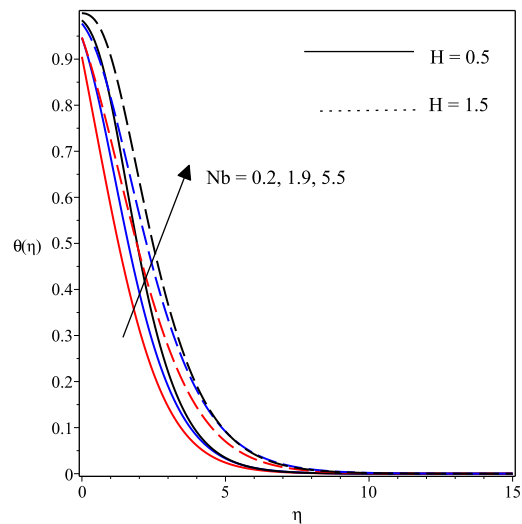
9

This plot signifies that enhancing Q raises the temperature profile due to additional heat generated to the stretching sheet by the imposition of Q. It is shown in Fig. 9 that a hike in the magnitude of N_b enhances the thermal field. The trend for the magnetic field parameter H on the temperature behaves similarly to that of N_b.

Magnetic field impact offers additional heating to the fluid due to the resistance to the fluid motion created by the Lorentz force.

Fig. 10 illustrates the influence of thermal slip parameter G_2 and thermophoresis N_t on the temperature profile.
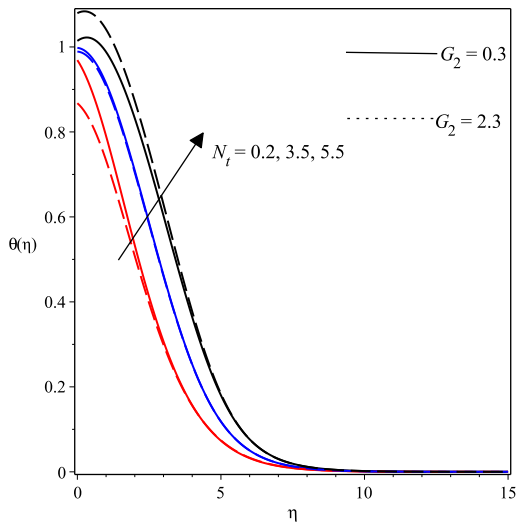
Fig. 10. Impact of N_t and G_2 on $\theta(\eta)$ **Fig. 11. Influence of Da and Ec on $\theta(\eta)$**
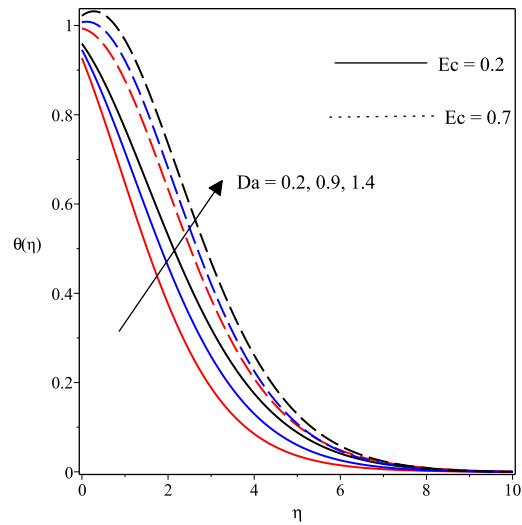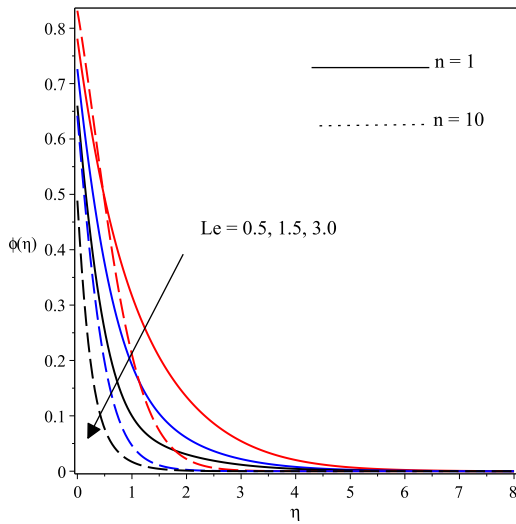
Fig. 12. Impact of Le and n on $\phi(\eta)$ **Fig. 13. Influence of K_r and N_b on $\phi(\eta)$**
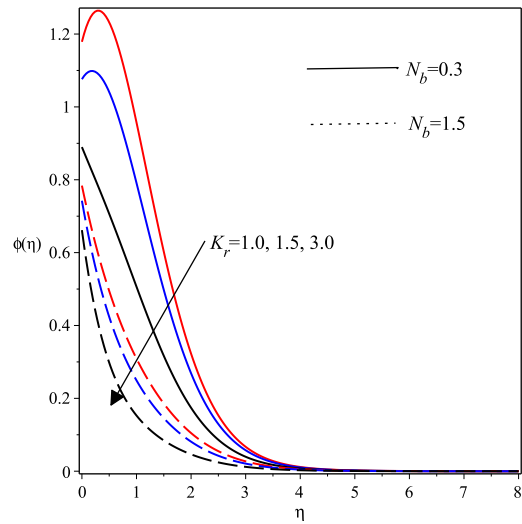
It can be observed that the temperature field lowers significantly with a rise in the magnitude of G_1 whereas with an increase in N_t, the thermal field expands. An increase in the Da also facilitates a growth in the temperature profile as displayed in Fig. 11. The resistance created to the fluid flow by the permeability of the porous medium then leads to the generation of heat which triggers a growth in the temperature. Furthermore, in Fig. 11, viscous dissipation effect depicted by Eckert number Ec raises the temperature distribution owing to the extra heat generated by the drag between the sheet and the fluid particles. The impact of Lewis number Le and nonlinear stretching n parameter on the concentration of nanoparticles is depicted in Fig. 12. This graph indicated that increasing values of Le act to reduce the nanoparticle concentration. In Fig. 13, a rise in the chemical reaction term K_r as well as that of Brownian motion N_b leads to a decline in the concentration.

5   CONCLUSIONS

A numerical investigation of hydromagnetic radiative Casson nanofluid transport is investigated over a nonlinear vertically stretchable surface confined in a porous medium. The flow is characterized by multiple slip properties with heat source together with viscous dissipation and homogeneous chemical reaction. The dimensionless equations describing the problem are solved numerically via shooting techniques in conjunction with the Runge-Kutta Fehlberg integration scheme. At the same time, the impact of the emerging physical terms relative to the problem are graphically described and deliberated. Besides, the underlisted facts are deduced from the analysis.

- An upsurge in the value of Grashof number G_r, Eckert Ec as well as G_c generates a significant rise in the motion of the fluid. In contrast, a rise in Casson material term β, nonlinear stretching term n and velocity slip factor G_1 decelerate the fluid motion.
- The thermal field is raised with growth in the magnitude of radiation parameter N_r, Eckert number Ec, thermophoresis term N_t, Brownian movement N_b, heat

source Q and magnetic field H whereas it decreases with a rise temperature slip term G_2.
- Rising values of chemical reaction K_r, Brownian movement N_b as well as Lewis number Le lowers the field of concentration together with concentration boundary structure.

COMPETING INTERESTS

Authors have declared that no competing interests exist.

REFERENCES

[1] Ishak A, Nazar R, Pop I. Uniform suction/blowing effect on flow and heat transfer due to a stretching cylinder. Appl Math Model. 2008;32(10):5966.

[2] Tlili I, Khan WA, Khan I. Multiple slips effects on MHD SA-Al2O3 and SA-Cu non-Newtonian nanofluids flow over a stretching cylinder in porous medium with radiation and chemical reaction. Results in Physics. 2018;8:213222.

[3] Karra S, Prusa V, Rajagopal KR. Maxwell fluid with relaxation time and viscosity depending on pressure. International Journal of Non-Linear Mechanics. 2011;46(6):819-827.

[4] Ireka IE, Okoya SS. Analysis of unsteady flow of second grade fluid with power law spatially distributed viscosity. Afrika Matematika. 2020;31:11751191.

[5] Fatunmbi EO, Fenuga OJ. MHD micropolar fluid flow over a permeable stretching sheet in the presence of variable viscosity and thermal conductivity with Soret and Dufour effects. Int J Math Ana Optimization: Theory & Appll. 2017;211-232.

[6] Casson NA. Flow equation for the pigment oil suspensions of the printing ink type in rheology of disperse systems. Pergamon, New York. 1959;84-102.

[7] Mahmoud MAA. Slip velocity effect on a non-Newtonian power-law fluid over a moving permeable surface with

heat generation. Math Comput Modell. 2011;54:2837.

[8] Imran U, Shafie S, Khan I. Effects of slip condition and Newtonian heating on MHD flow of Casson fluid over a nonlinearly stretching sheet saturated in a porous medium. Journal of King Saud University; 2016.
Available:http://dx.doi.org/10.1016/j.jksus.2016.05.003

[9] Shaw S, Mahanta G, Sibanda P. Non-linear thermal convection in a Casson fluid flow over a horizontal plate with convective boundary condition. Alexandria Engineering Journal. 2016;55(2):12951304.

[10] Asogwa KK, Ibe AA. A study of MHD Casson fluid flow over a permeable stretching sheet with heat and mass transfer. Journal of Engineering Research and Reports. 2020;10-25.
DOI: 10.9734/jerr/2020/v16i217161.

[11] Shamshuddin MD, Mishra SR, Thumma T. Chemically reacting radiative Casson fluid over an inclined porous plate: A numerical study. In Numerical Heat Transfer and Fluid Flow. Springer, Singapore. 2019;469-479.

[12] Choi SUS. Enhancing thermal conductivity of fluids with nanoparticles. ASME International Mechanical Engineering Congress and Exposition. 1995;66:99105.

[13] Lee S, Choi SU, Li S, Eastman JA. Measuring thermal conductivity of fluids containing oxide nanoparticles. Journal of Heat Transfer. 1999;121(2):280289.

[14] Buongiorno J. Convective transport in nanofluids. Journal of Heat Transfer. 2006;128(3):240250.

[15] Aybar HS, Sharifpur M, Azizian MR, Mehrabi M, Meyer JP. A review of thermal conductivity models for nanofluids. Heat Transfer Engineering. 2015;36(13):10851110.

[16] Okonkwo EC, Wole-Osho I, Almanassra IW, et al. An updated review of nanofluids in various heat transfer devices. J Therm Anal Calorim; 2020.
Available:https://doi.org/10.1007/s10973-020-09760-2

[17] Abdelmalek Z, Hussain A, Bilald S, Sherif EM, Thounthong P. Brownian motion and thermophoretic diffusion influence on thermophysical aspects of electrically conducting viscoinelastic nanofluid flow over a stretched surface. Journal of Materials Research and Technology. 2020;9(5):11948-11957.

[18] Makinde OD, Mabood F, Khan WA, Tshehla MS. MHD flow of a variable viscosity nanofluid over a radially stretching convective surface with radiative heat. Journal of Molecular Liquids. 2016;219:624630.

[19] Alreshidi NA, Shah Z, Dawar A, Kumam P, Shutaywi M, Watthayu M. Brownian motion and thermophoresis effects on MHD three dimensional nanofluid flow with slip conditions and Joule dissipation due to porous rotating disk. Journal List Molecules. 2017;25(3).
DOI: 10.3390/molecules25030729

[20] Ashraf K, Siddique I, Hussain A. Impact of thermophoresis and Brownian motion on non-Newtonian nanofluid flow with viscous dissipation near stagnation point. Physica Scripta. 2020;95(5).

[21] Fatunmbi EO, Adeosun AT. Nonlinear radiative Eyring-Powell nanofluid flow along a vertical Riga plate with exponential varying viscosity and chemical reaction. International Communications in Heat and Mass Transfer. 2020;119:104913.

[22] Navier CLMH. Memoire sur les lois du mouvement des fluides. Memoires de Academie Royale des Sciences de Institut de France. 1823;6:389440.

[23] Rashad A. Unsteady nanofluid flowover an inclined stretching surface with convective boundary condition and anisotropic slip impact. International Journal of Heat and Technology. 2017;35(1):8290.

[24] Afify AA, Uddin MJ, Ferdows M. Scaling group transformation for MHD boundary layer flow over permeable stretching sheet in presence of slip flow with Newtonian heating effects. Applied Mathematics and Mechanics. 2014;35(11):13751386.

[25] Uddin MJ, Khan WA, Ismail AIM. Effect of variable properties, Navier slip and convective heating on hydromagnetic transport phenomena. Indian Journal of Physics. 2016;90(6):627637.

[26] Fatunmbi EO, Fenuga OJ. Heat and mass transfer of a chemically reacting MHD micropolar fluid flow over an exponentially stretching sheet with slip effects. Physical Science International Journal. 2018;18(3):1-15.

[27] Fatunmbi EO, Adeniyan A. Heat and mass transfer in MHD micropolar fluid flow over a stretching sheet with velocity and thermal slip conditions. Open Journal of Fluid Dynamics. 2018;8:195-215.
Available:https://doi.org/10.4236/ojfd.2018.82014

[28] Mukhopadhyay S, Gorla RSR. Effects of partial slip on boundary layer flow past a permeable exponential stretching sheet in presence of thermal radiation. Journal of Heat and Mass Transfer; 2012.
Available:http://dx.doi.org/10.1007/s00231-012-1024-8 [in press].

[29] Jamaludin A, Naganthran K, Nazar R, Pop I. Thermal radiation and MHD effects in the mixed convection flow of ferrofluid towards a nonlinearly moving surface. Processes. 2020;8.
DOI: 10.3390/pr8010095.

[30] Zaidi HN, Yousif M, Nasreen SN. Effects of thermal radiation, heat generation, and induced magnetic field on hydromagnetic free convection flow of couple stress fluid in an isoflux-isothermal vertical channel; 2020. article ID 4539531.
Available:https://doi.org/10.1155/2020/4539531

[31] Bhandari A. Radiation and chemical reaction effects on Nanofluid flow over a stretching sheet. Journal of Fluid Dynamics and Material Processing. 2019;15(5):557-582. doi:10.32604/fdmp.2019.04108.

[32] Abd El-Aziz M. Effect of time-dependent chemical reaction on stagnation point flow and heat transfer over a stretching sheet in a nanofluid. Physica Scripta. 2014;89(8):085205.
DOI: 10.1088/0031-8949/89/8/085205

[33] Fatunmbi EO, Adeniyan A. MHD stagnation point flow of micropolar fluids past a permeable stretching plate in porous media with thermal radiation, chemical reaction and viscous dissipation. Journal of Advances in Mathematics and Computer Science. 2018;26(1):1-19. Tretching Sheet in a Nanofluid. Physica Scripta. 89(8), article ID085205.

[34] Eid MR. Chemical reaction effect on MHD boundary layer flow of two-phase nanofluid model over an exponentially stretching sheet with a heat generation. Journal of Molecular Liquids. 2016;220:718725.

[35] Afify AA, Elgazery NS. Effect of a chemical reaction on magnetohydrodynamic boundary layer flow of a Maxwell fluid over a stretching sheet with nanoparticles. Particuology. 2016;29:154161.

[36] Rashidi MM, Ali M, Rostami B, Rostami P, Xie G. Heat and mass transfer for MHD Viscoelastic Fluid flow over a vertical stretching sheet with considering Soret and Dufour effects. Mathematical Problems in Engineering; 2015. Article ID 861065, 12 pages.
Available:http://dx.doi.org/10.1155/2015/861065

[37] Jabeen K, Mushtaq M, Akram RM. Numerical simulation of MHD boundary layer flow and heat transfer over a nonlinear stretching sheet in the porous medium with viscous dissipation using hybrid approach. Mathematical Problems in Engineering. 2020;1-9.

[38] Fatunmbi EO, Okoya SS. Quadratic mixed convection stagnation-point flow in hydromagnetic Casson nanofluid over a nonlinear stretching sheet with variable thermal conductivity. Defect and Diffusion Forum Submitted. 2020;409:95-109.

[39] Jafar AB, Shafie S, Ullah I. MHD radiative nanofluid flow induced by a nonlinear stretching sheet in a porous medium. Heliyon. 2020;6:e04201.

[40] Yazdi MH, Abdulaah S, Hashim I, Sopian K. Effects of viscous dissipation on the slip MHD flow and heat transfer past a permeable surface with

convective boundary conditions. Energies. 2011;4:22732294.

[41] Fatunmbi EO, Okoya SS, Makinde OD. Convective heat transfer analysis of hydromagnetic micropolar fluid flow past an inclined nonlinear stretching sheet with variable thermophysical properties. Diffusion Foundations. 2019;26:63-77.

[42] Gbadeyan JA, Titiloye EO, Taofeeq A. Effect of variable thermal conductivity and viscosity on Casson nanofluid flow with convective heating and velocity slip. Heliyon. 2020;6(1):e03076.
DOI: 10.1016/j.heliyon.2019.e03076.

[43] Animasaun IL, Adebile EA, Fagbade AI. Casson fluid flow with variable thermo-physical property along exponentially stretching sheet with suction and exponentially decaying internal heat generation using the homotopy analysis method. Journal of the Nigerian Mathematical Society. 2016;35(1):1-17.

[44] Raza J, Farooq M, Mebarek-Oudina F, Mahanthesh B. Multiple slip effects on MHD non-Newtonian nanofluid flow over a nonlinear permeable elongated sheet. Multidiscipline Modeling in Materials and Structure. 2019;15(5):913-931.

[45] Attili BS, Syam ML. Efficient shooting method for solving two point boundary value problems. Chaos, Solitons and Fractals. 2008;35(5):895903.

[46] Mahanthesh B, Gireesha BJ, Gorla RSR, Makinde OD. Magnetohydrodynamic three-dimensional flow of nanofluids with slip and thermal radiation over a nonlinear stretching sheet: a numerical study, Neural Computing and Applications. 2018;30(5):15571567.

[47] Fatunmbi EO, Okoya SS. Heat transfer in boundary layer magneto-micropolar fluids with temperature-dependent material properties over a stretching sheet. Advances in Materials Science and Engineering; 2020. Article ID 5734979, 1-11.

[48] Megahed AM. Williamson fluid flow due to a nonlinearly stretching sheet with viscous dissipation and thermal radiation, Journal of the Egyptian Mathematical Society. 2019;27(12):1-10.
Available:https://doi.org/10.1186/s42787-019-0016-y

[49] Gorla RSR, Sidawi I. Free convection on a vertical stretching surface with suction and blowing. Appl. Sci. Res. 1994;52:47257.